Neurobiology of Aging 69 (2018) 140–150

Contents lists available at ScienceDirect

Neurobiology of Aging

journal homepage: www.elsevier.com/locate/neuaging

Functional networks underlying item and source memory: shared and distinct network components and age-related differences

Zachary A. Monge [a,*], Matthew L. Stanley [a], Benjamin R. Geib [a], Simon W. Davis [a,b], Roberto Cabeza [a]

[a] Center for Cognitive Neuroscience, Duke University, Durham, NC, USA
[b] Department of Neurology, Duke University School of Medicine, Durham, NC, USA

ARTICLE INFO

Article history:
Received 16 November 2017
Received in revised form 30 April 2018
Accepted 14 May 2018
Available online 21 May 2018

Keywords:
Aging
Functional connectivity
Graph theory
Memory
Modularity

ABSTRACT

Although the medial temporal lobes (MTLs) are critical for both *item memory* (IM) and *source memory* (SM), the lateral prefrontal cortex and posterior parietal cortex play a greater role during SM than IM. It is unclear, however, how these differences translate into *shared* and *distinct* IM versus SM network components and how these network components vary with age. Within a sample of younger adults (YAs; n = 15, M_{age} = 19.5 years) and older adults (OAs; n = 40, M_{age} = 68.6 years), we investigated the functional networks underlying IM and SM. Before functional MRI scanning, participants encoded nouns while making either pleasantness or size judgments. During functional MRI scanning, participants completed IM and SM retrieval tasks. We found that MTL nodes were similarly interconnected among each other during both IM and SM (*shared* network components) but maintained more intermodule connections during SM (*distinct* network components). Also, during SM, OAs (compared to YAs) had MTL nodes with more widespread connections. These findings provide a novel viewpoint on neural mechanism differences underlying IM versus SM in YAs and OAs.

1. Introduction

Abundant evidence supports the distinction between 2 fundamental forms of episodic memory—item memory (IM) and source memory (SM) (for reviews, see Eichenbaum et al., 2007; Skinner and Fernandes, 2007; Vilberg and Rugg, 2008; Wais, 2008; Wixted, 2007). IM refers to the memory for *what happened*, which in the laboratory corresponds to the memory for specific experimental stimuli (e.g., that I had met this person). In contrast, SM refers to the memory for *where, when, and how an event happened*, which in the laboratory corresponds to the memory for spatial, temporal, semantic, and/or perceptual contexts of experimental stimuli (e.g., the location where I met this person). Considerable research investigating the neural correlates of IM and SM has suggested that both IM and SM are dependent on the *medial temporal lobes* (MTLs), whereas SM (compared to IM) is additionally more dependent on the *lateral prefrontal cortex* (LatPFC) and *posterior parietal cortex* (PPC; for a review, see Mitchell and Johnson, 2009).

The observation that both IM and SM recruit MTL regions (e.g., Davachi et al., 2003; Hayes et al., 2011; Staresina and Davachi, 2008, 2009), whereas SM typically also recruits LatPFC and PPC (e.g., Cabeza et al., 2008; Dobbins et al., 2003; Giovanello and Schacter, 2012; Hayes et al., 2011; Kim, 2013; Spaniol et al., 2009; Vilberg and Rugg, 2007; Wheeler and Buckner, 2004), is largely based on univariate activation analyses. Although these studies have provided important information on the neural correlates of IM and SM, a critical limitation of univariate activation analyses is that they only identify the contributions of individual, encapsulated regions without reference to how those regions are situated within the larger system. That is, the activations of individual brain regions tell only part of the story because any cognitive process, including memory, depends not only on individual regions but also on how brain regions *interact* with each other (Telesford et al., 2011; van den Heuvel and Sporns, 2013). For example, LatPFC and PPC regions recruited during SM are assumed to interact very closely with the MTL (for a review, see Mitchell and Johnson, 2009). Thus, the difference between SM and IM may not merely be that SM requires additional LatPFC and PPC recruitment but also that these specific regions interact with other network components, such as the MTL. Indeed, preliminary evidence indicates that during SM, MTL regions are functionally connected to LatPFC and PPC (e.g., Foster et al., 2016; McCormick et al., 2010), but this literature is limited in that

* Corresponding author at: Duke University, Levine Science Research Center, Center for Cognitive Neuroscience, Box 90999 Durham, NC 27708 USA. Tel.: +1 919 668 2299; fax: +1 919 681 0815.
E-mail address: zachary.monge@duke.edu (Z.A. Monge).

0197-4580/$ – see front matter © 2018 Elsevier Inc. All rights reserved.
https://doi.org/10.1016/j.neurobiolaging.2018.05.016

past studies have almost exclusively examined bivariate functional connectivity. A more complete description of the functional connectivity patterns underlying IM and SM may be derived from *multivariate functional connectivity analyses*, which allow for the examination of complex, whole-brain functional networks underlying cognition.

This investigation is especially relevant within the study of cognitive aging, where age-related memory deficits are about twice as large in SM than in IM (Spencer and Raz, 1995). Indeed, these age-related differences in SM appear to be associated with changes in the neural correlates of SM, where, in general, older adults (OAs) compared to younger adults (YAs) exhibit increased LatPFC and PPC activation during SM (Dulas and Duarte, 2012; Leshikar et al., 2010; Spaniol and Grady, 2012). However, like the studies within YAs, these findings were predominantly based on univariate activation analyses. A preliminary functional connectivity study demonstrated that during SM, OAs (compared to YAs) exhibited greater functional connectivity between the hippocampus (HC) and prefrontal cortex, whereas YAs (compared to OAs) exhibited greater functional connectivity between the HC and posterior occipitotemporal regions (Dennis et al., 2008), but this study only examined bivariate functional connectivity. As such, this analysis relied on connectivity patterns centered around the HC—an important region but nonetheless only one brain region. It remains unknown how large-scale functional networks vary with age during IM and SM.

Here, we used graph theoretical-multivariate functional connectivity analyses to examine in a sample of YAs and OAs the functional networks underlying IM and SM. We characterized these connectivity patterns with *graph metrics* estimated from functional whole-brain networks (for reviews, see Bullmore and Sporns, 2009; van den Heuvel and Sporns, 2013). A functional brain network comprises brain regions (known as *nodes*) and the functional interactions between brain regions (known as *edges*). Graph metrics allow for the characterization of complex patterns of interactions in the network. We specifically examined IM compared to SM *shared* and *distinct* MTL functional connectivity patterns irrespective of age and also by comparing YAs and OAs. Although univariate activation analyses have identified shared and distinct activation patterns between IM and SM (e.g., Giovanello and Schacter, 2012; Hayes et al., 2011; Spaniol et al., 2009; Vilberg and Rugg, 2007), this is the first study, to our knowledge, to characterize these components within a whole-brain functional network framework.

In particular, we focused on the graph metric of *modularity*, which identifies, in a data-driven manner, regions (or nodes) that form tightly interconnected subgroups (i.e., modules; for reviews, see Mišić and Sporns, 2016; Sporns and Betzel, 2016; Telesford et al., 2011). Modules do not function in isolation, and both the links between modules and the links within modules contribute to cognition (Cohen and D'Esposito, 2016; Davis et al., 2017; Grady et al., 2016; Stanley and Brigard, 2016). Several recent studies have demonstrated that modular properties of brain networks shift in response to cognitive demands of the environment (e.g., Cohen and D'Esposito, 2016; Geib et al., 2017a; Monge et al., 2018) and change across the lifespan (e.g., Betzel et al., 2014; Chan et al., 2014, 2017; Gallen et al., 2016; Geerligs et al., 2015; Grady et al., 2016; Monge et al., 2017), making the investigation of these properties worth studying in cognitive aging. To our knowledge, no study has investigated the functional-modular topology underlying IM and SM.

In the present study, before scanning, YAs and OAs encoded concrete words while making either pleasantness or size judgments (to serve as the source). During functional MRI (fMRI) scanning, memory for the studied words was tested in separate IM and SM retrieval tests, and network analyses were used to characterize the functional network topology of the IM and SM networks. Our overarching goal was to characterize, both irrespective of age and accounting for age-related differences, the functional network topology of the IM and SM networks. We had 3 main predictions. First, based on evidence that both IM and SM are dependent on the MTL, whereas SM also depends on the LatPFC and PPC (for a review, see Mitchell and Johnson, 2009), we predicted that *MTL module-inside functional connections would be similar for the IM and SM networks* (*shared network components*), *whereas MTL module-outside functional connections, particularly between the HC and LatPFC/PPC, would be stronger for SM than IM* (*distinct network components*; first prediction). Second, based on work demonstrating that a more integrated functional network is associated with better performance on more complex cognitive tasks (e.g., Backus et al., 2016; Barbey, 2018; Geib et al., 2017a,b; Grady et al., 2016; Meunier et al., 2014; Monge et al., 2017; Stanley et al., 2015; van den Heuvel et al., 2009), we predicted that *controlling for age group, within the SM network, a greater proportion of MTL module-outside than MTL module-inside connections would be associated with better SM task performance* (second prediction). Third, based on evidence that increased age is associated with (1) a greater decline in SM than IM (for a review, see Spencer and Raz, 1995) and (2) increased SM-related brain activity (Dulas and Duarte, 2012; Leshikar et al., 2010; Spaniol and Grady, 2012), we predicted that *in the SM network, OAs* (*compared to YAs*) *would show more MTL module-outside than MTL module-inside connections* (third prediction).

2. Methods

2.1. Study sample

A total of 16 healthy YAs and 52 healthy OAs completed all sessions of our study. All participants were right-handed and native English speakers. The YAs and OAs were screened via a self-report questionnaire for neurological and psychiatric conditions, and the OAs were additionally screened via the modified Mini-Mental State Examination (exclusion criterion score <27; Bravo and Hébert, 1997; Folstein et al., 1975) for possible cognitive dysfunction. Based on these criteria, no exclusions were necessary. However, 1 YA and 12 OAs were excluded from our analyses for at least one of the following reasons: computer-related error during encoding, scanner-related malfunction, excessive head motion during the fMRI session (several "spikes" of movement in any direction greater than 3 mm), missing data, and/or MTL nodes becoming severely fractured after thresholding their connectivity matrices (see Section 2.5 for more details). This left a study sample of 15 YAs and 40 OAs. The YAs were 18–22 years old ($M = 19.5$, standard deviation [SD] = 1.3) and the OAs were 61–87 years old ($M = 68.6$, $SD = 6.4$). The Duke University Institutional Review Board approved all experimental procedures, and participants provided informed consent before testing.

2.2. IM and SM tasks

2.2.1. Encoding

Outside of the scanner, participants intentionally studied 440 English words (e.g., *man*, *watch*, *jar*). Stimuli were presented in MATLAB (MathWorks, Natick, MA, USA), and stimulus presentation was on a 19-inch computer monitor, displayed in black font on a gray background for 3 seconds with a 1-second intertrial interval. Words had normative word frequencies in the lexicon of 5–15 per million ($M = 8.8$, $SD = 3.1$) and a mean length of 7.1 ($SD = 2.3$) letters (Francis and Kucera, 1967). On half of trials, participants made "pleasant/unpleasant" judgments and the other half "bigger/smaller than a shoebox" judgments. Participants were asked to make these

judgments to later test the context in which the word was presented (i.e., SM). The words were presented within 4 encoding lists, which each consisted of 50 words presented twice and 40 words presented 4 times (total of 260 trials per encoding list). For each participant, the words presented within each encoding list were randomly generated. Participants intentionally encoded both the words and the judgment associated with each word, and they were aware that some of the words would be repeated. Before the scan session, participants completed a short practice test (10 items) of the encoding, IM retrieval, and SM retrieval tasks.

2.2.2. Retrieval

Approximately 15 minutes after the encoding phase, participants were placed in the MRI scanner and completed the retrieval phase. Over 8 runs, participants completed 2 retrieval run types—4 IM and 4 SM retrieval runs. During the IM retrieval runs, participants were presented words individually and made old/new responses on a 4-point confidence scale—definitely old, probably old, probably new, and definitely new. For each IM run, participants were presented 45 targets (studied words) and 20 lures (non-studied words). During the SM retrieval runs, participants were presented old words individually and made SM judgments on the trial type in which the word was originally studied on a 4-point scale—definitely pleasant/unpleasant, probably pleasant/unpleasant, probably bigger/smaller than a shoebox, and definitely bigger/smaller than a shoebox. Because participants were informed that all words were previously presented during encoding, the SM task was designed to only test the context in which the word was previously studied (i.e., SM). For each SM run, participants were presented 45 studied words. All retrieval stimuli were presented for 3 seconds followed by a jittered interstimulus interval (1–7 seconds) with a white fixation cross on a black background. Stimuli were presented with a mirror in the scanner head coil and a rear projection system. Participants used a 4-key fiber-optic response box (Resonance Technology, Inc) to make behavioral responses. Participants with corrected vision used MRI-compatible lenses.

2.3. MRI data acquisition

A General Electric 3T Signa Excite HD short bore scanner and 8-channel head coil were used to collect functional and anatomical images. Coplanar functional images were acquired with an inverse spiral sequence (64 × 64 matrix, repetition time [TR] = 1700 ms, echo time [TE] = 31 ms, field of view [FOV] = 240 mm, 37 slices, 3.8 mm slice thickness, 254 images) using a spiral-in gradient-echo sequence (slice order = interleaved, 64 × 64 matrix, TR = 2000 ms, TE = 27 ms, sections = 34, thickness = 3.8 mm, interscan spacing = 0, flip angle = 60°, SENSE reduction factor = 2). Following, a high-resolution spoiled gradient recalled series (1 mm sections covering whole brain, interscan spacing = 0, matrix = 256 × 256, flip angle = 30°, TR= 2 ms, TE = min full, FOV = 19.2 cm) and a high-resolution anatomical image using a 3D T_1-weighted echo-planar sequence (matrix = 256 × 256, TR = 12 ms, TE = 5 ms, FOV = 24 cm, slices = 68, slice thickness = 1.9 mm, sections = 248) were collected. Total scan time, including breaks, was approximately 1 hour and 40 minutes.

2.4. fMRI analysis

2.4.1. Preprocessing

The first 4 images of each run were discarded to allow for scanner equilibrium. The functional images were preprocessed within an SPM12 (London, UK; http://www.fil.ion.ucl.ac.uk/spm/) pipeline. Briefly, functional images were slice timing corrected (reference slice = first slice), realigned to the first scan in the first run, and subsequently unwarped. Following, the functional images were coregistered to the skull-stripped T1 image (skull-stripped by segmenting the T1 image and only including the gray matter, white matter, and cerebrospinal fluid segments) and subsequently normalized to Montreal Neurological Institiute space (voxel size was maintained at 3.75 × 3.75 × 3.8 mm^3). The functional images were then spatially smoothed using an 8 mm Gaussian kernel. For the functional images, we also ensured there were not any TRs with excessive motion (relative to start of run motion >2.5 mm or degrees in any direction; Madden et al., 2017; Monge et al., 2017); there were no TRs with excessive motion.

2.4.2. IM and SM network construction

To examine the functional network topology underlying IM and SM, for each participant, we constructed separate IM and SM functional connectivity matrices. The functional connectivity matrices were constructed using a correlational psychophysiological interaction approach (Fornito et al., 2012). Briefly, for each region of interest (ROI; i.e., node), the correlational psychophysiological interaction relies on the calculation of a PPI term, which is based on the product of (1) that ROI's average time course and (2) a task regressor of interest (i.e., the specified experimental manipulation). For this study, the ROIs were derived from the cortical, HC, and amygdala ROIs (separately for the left and right hemispheres) of the Harvard-Oxford Probabilistic Atlas (a total of 100 ROIs; Desikan et al., 2006). Although the choice of atlas may influence the topological properties of a brain network (Stanley et al., 2013), the Harvard-Oxford Atlas has been used in many previous graph theoretical-functional connectivity studies (e.g., Bassett et al., 2011; Cohen and D'Esposito, 2016; Wang et al., 2011). For our study, we implemented this nodal partitioning scheme to better differentiate and investigate subregions of the MTL (6 MTL nodes), compared to the also commonly used automated anatomical labeling atlas (Tzourio-Mazoyer et al., 2002), which only contains 4 MTL nodes. The task regressor was created separately for the IM and SM runs, and it comprised a convolved hemodynamic response with stick functions for remembered, high confidence trials (i.e., high confidence hits); for this study, we only examined hits because (1) many participants had too few miss trials and (2) the goal of the study was to compare IM and SM to each other. All other trial types were modeled but not used in the connectivity analysis. This convolved task response vector was multiplied by the time course of each ROI within the appropriate run (IM or SM) yielding for each run type a PPI term. For each run type, the PPI term of each ROI was multiplied with the PPI term of every other ROI yielding partial correlations between ROIs: $\rho PPI_i, PPI_{j.z}$, where i and j represent example ROIs, and z represents the controlled variance associated with the task regressor, the time courses for regions i and j, constituent motion regressors (6 motion parameters), the white matter time series regressor, and the cerebrospinal fluid time series regressor. The white matter and cerebrospinal fluid time series were derived from the white matter and cerebrospinal fluid segments (for each segment, only including voxels with greater than 99% probability of either including the white matter or cerebrospinal fluid). This analysis yielded, for each participant, 2 separate weighted, undirected functional connectivity matrices (100 × 100 nodes), representing the networks of interest—an IM network and SM network.

2.4.3. IM and SM network modularity and graph metric analysis

A modularity analysis, using the Louvain algorithm (Blondel et al., 2008; Rubinov and Sporns, 2010), was conducted to examine the modular architecture of the IM and SM networks. For the modularity analysis, first, we created participant-averaged IM- and SM-weighted connectivity matrices. We then thresholded each averaged connectivity matrix to include only the strongest subset of

connections (i.e., highest correlation coefficients) using a procedure developed by Hayasaka and Laurienti (2010). Briefly, edge density between the averaged IM and SM networks was matched using the formula $N = K^S$, with N equal to the number of nodes, K equal to the average degree, and S set to 2.0; this thresholding procedure yields graphs with a density of 0.20. This method has been usefully implemented in many different task-related network analyses of fMRI data, and it provides a means of making different network properties appropriately comparable between conditions (e.g., Stanley et al., 2014, 2015). This particular threshold (i.e., $S = 2.0$) was chosen for 2 main reasons. First, when S was set to a value greater than 2.0, these networks severely fragmented, which makes it difficult to interpret and compare the topological properties of these networks. Second, prior research has indicated that when S is equal to or between 2 and 3, brain networks tend to be more reproducible (Telesford et al., 2013). Those edges between any 2 given nodes that met the threshold requirement were assigned a value of 1, and all other edges were assigned a value of 0. This resulted in 2 averaged, thresholded matrices—an averaged IM adjacency matrix and averaged SM adjacency matrix.

For the averaged IM and SM adjacency matrices, we estimated modularity using the Louvain algorithm. The Louvain algorithm was applied to each averaged, thresholded adjacency matrix 1000 times (Geib et al., 2017a). The outputs of the Louvain algorithm modularity analysis are the community partition (the module assignment for each node) and the Q-value. The Q-value indicates how well the algorithm is able to segregate a network into modules, where higher values indicate that a network has a more distinctive, segregated modular architecture. The best partition, taken separately for the IM and SM networks, was identified as the run that produced the highest Q-value, and this partition was used for all subsequent analyses. For the modularity analysis, all study participants (n = 55) were included. The only exception to this was when testing our third prediction (see Section 3.4), in which we used age group–specific modules (similar to Chan et al., 2017). To estimate participant-specific Q-values (see Section 3.4), the Louvain algorithm was applied 1000 times to each participant's unique thresholded IM and SM adjacency matrices, and the run that produced the highest Q-value (separate for the IM and SM adjacency matrices) was chosen as the participant's Q-value. For nodes contained within modules, we calculated the relative number of outside- to inside-module connections by calculating the graph metric *participation coefficient* (Guimera and Amaral, 2005); higher values indicate more outside- than inside-module connections (i.e., a more *integrated* rather than *segregated* topology). It should be noted that although participation coefficient may be calculated for an individual node, this measure takes into consideration functional connections throughout the entire network, as participation coefficient is essentially the ratio of outside- to inside-module connections. All graph metrics were calculated using scripts publicly available within the Brain Connectivity Toolbox (Rubinov and Sporns, 2010).

2.5. Statistical testing

Participants' behavior and graph metric measures were analyzed with linear mixed effects models conducted within Statsmodels 0.6.1 (Seabold and Perktold, 2010) ran in Python 3.4.5 (Python Software Foundation, https://www.python.org/). For behavior, to test our second prediction (see Section 3.3), our main behavioral outcome measure was scaled reaction time (RT; median RT/accuracy) to account for speed-accuracy tradeoffs (Boldini et al., 2007; Dosher, 1976; Horowitz and Wolfe, 2003; Madden et al., 2017; Smith and Brewer, 1995; Starns and Ratcliff, 2010; Townsend and Ashby, 1983). For the graph metric measures, linear mixed effects models were used to assess interaction effects, and post hoc comparisons (for statistically significant interactions) were examined using a modified permutation test (Simpson et al., 2013) in conjunction with the Jaccardized Czekanowski index (Schubert, 2013; Schubert and Telcs, 2014) that was created specifically for pair-wise comparisons in graph theoretic brain network analyses. This procedure was recently implemented to investigate differences in the topological properties of task-related brain networks between conditions of interest (Geib et al., 2017a,b; Stanley et al., 2014).

For all analyses in which participant-specific graph metrics were estimated from participant-specific adjacency matrices, the matrices were thresholded using the previously described procedure (see Section 2.4.3; Hayasaka and Laurienti, 2010). Because we were specifically interested in the MTL, after thresholding, we excluded participants in which 3 or more MTL nodes became fractured from either the IM or SM network because it is difficult to interpret and compare topological properties of brain networks when some networks are fractured and others are not. Based on this criterion, 1 YA and 2 OAs were excluded. We believe that the fractured MTL nodes within these 3 participants may have been caused by low signal-to-noise ratio (SNR) within the MTL. Indeed, during the IM runs, within the 3 excluded participants, the SNR within the MTL (averaged across the 6 MTL ROIs) was below the sample average. During the SM runs, within one of the excluded participants, the SNR within the MTL was below the sample average and, within another excluded participant, the SNR was below the sample average in 2 MTL nodes. Also, for the analysis examining functional connections between the HC, LatPFC and PPC (see Section 3.2), nodes from the LatPFC included bilateral superior frontal gyri and from the PPC included bilateral superior parietal lobule; we chose these nodes because (1) previous work has identified the LatPFC and PPC to be involved in SM (e.g., Giovanello and Schacter, 2012; Hayes et al., 2011; Spaniol et al., 2009; Vilberg and Rugg, 2007), and (2) we hypothesized that SM would be most dependent on frontoparietal regions associated with top-down/executive function processing (Bunge et al., 2004; Cabeza et al., 2008; Dobbins et al., 2002). Finally, for any analysis describing participation coefficient results for a set of nodes (e.g., the 6 MTL nodes), participation coefficient was calculated for each node in the set and then averaged across those nodes. BrainNet Viewer was used to overlay results on a brain surface (Xia et al., 2013).

3. Results

3.1. IM and SM task performance

Participants' task performance is reported in Table 1. Overall, participants had lower accuracy on the SM than IM task (high confidence IM $M = 0.71$, $SD = 0.17$ proportion of hits; high confidence SM $M = 0.59$, $SD = 0.17$ proportion of hits; $\beta = -0.12$, $z = 7.12$, $p < 0.0001$). Also, participants responded faster on the IM than SM task (high confidence IM $M = 1319.1$ ms, $SD = 302.3$ ms; high confidence SM $M = 2080.2$ ms, $SD = 528.1$ ms; $\beta = 761.1$, $z = 14.62$, $p < 0.0001$). Finally, scaled RTs were lower during the IM than SM task (high confidence IM $M = 2078.2$, $SD = 1011.8$ ms; high confidence SM $M = 4232.6$ ms, $SD = 2810.7$ ms; $\beta = 2154.4$, $z = 7.38$, $p < 0.0001$). Also, between the age groups, accuracy and scaled RTs were similar (both z's < 0.71, p's > 0.48), but for RT, the OAs ($M = 1779.1$ ms, $SD = 609.6$ ms) compared to YAs ($M = 1487.8$ ms, $SD = 403.3$ ms) had higher RTs ($\beta = 291.3$, $z = 2.42$, $p < 0.05$). The age group by task interaction was only significant for accuracy ($\beta = 0.11$, $z = 3.01$, $p < 0.01$), in which the IM-SM task accuracy difference was greater within the YAs (IM-SM high confidence accuracy: $M = 0.20$, $SD = 0.13$; $t\,[14] = 5.94$, $p < 0.0001$) than OAs (IM-SM high confidence accuracy: $M = 0.09$, $SD = 0.11$; $t\,[39] = 5.14$, $p < 0.0001$).

Table 1
Task performance

Task	Younger adults *M* (*SD*)	Older adults *M* (*SD*)	95% CI lower limit, upper limit
Item memory			
Scaled RT (ms)	1809.2 (780.2)	2179.1 (1077.3)	162.4, 577.3[a]
RT (ms)	1186.6 (142.8)	1368.7 (331.6)	169.3, 194.9[b]
Accuracy	0.72 (0.17)	0.70 (0.17)	−0.024, −0.015[b]
Source memory			
Scaled RT (ms)	4277.0 (2813.0)	4215.9 (2845.6)	−359.5, 237.3
RT (ms)	1789.0 (349.5)	2189.4 (545.4)	293.4, 507.4[b]
Accuracy	0.52 (0.19)	0.61 (0.16)	0.022, 0.154[c]

All values represent performance for high confidence hits. Accuracy reflects the proportion of high confidence hit responses. The 95% CIs indicate age group differences.
Key: CI, confidence interval; *M*, mean; *SD*, standard deviation; RT, reaction time; scaled RT, RT/accuracy.
[a] $p < 0.001$.
[b] $p < 0.0001$.
[c] $p < 0.01$.

3.2. IM and SM network modularity analysis

Before testing our first prediction about IM versus SM in MTL module connectivity, we had to confirm the premise that both the IM and SM networks (1) exhibited a modular architecture and (2) contained a module that included most MTL nodes. Supporting the first premise, the modularity algorithm revealed that the IM network (Fig. 1A; Supplementary Table 1) contained 4 modules and the SM network (Fig. 1B; Supplementary Table 2) contained 5 modules. To quantitatively determine that each of these networks exhibited a modular architecture, the modularity algorithm was repeated 1000 times on nonrandomized versus randomized networks [constructed via a rewiring algorithm that preserves network density (Rubinov and Sporns, 2010)]. Both the nonrandomized IM ($p < 0.0001$, permutation test) and SM ($p < 0.0001$, permutation test) networks, compared to the density-matched randomized networks, had significantly higher *Q*-values, indicating that the IM and SM networks exhibited a modular architecture. Also, the IM network (*Q* range: 0.2732–0.3041) had lower *Q*-values than the SM network (*Q* range: 0.2952–0.3532; $p < 0.0001$, permutation test).

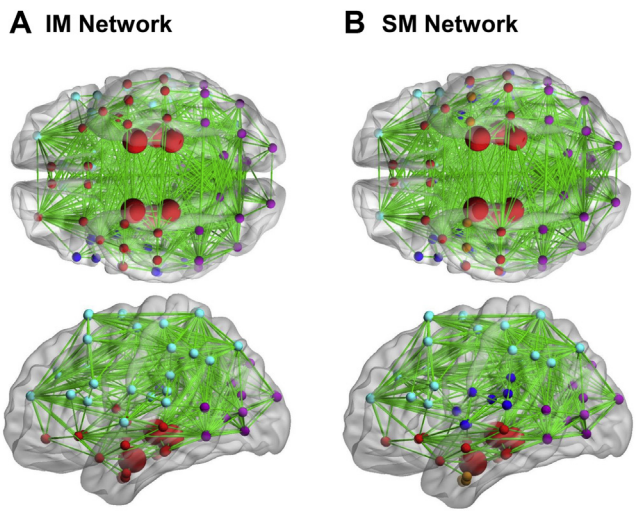

Fig. 1. Modular architecture of the IM and SM networks. Panel A shows the modules identified in the IM network, and Panel B shows the modules identified in the SM network. Both networks contained an MTL+ module including all 6 MTL nodes (large red spheres) and other nodes predominantly in lateral temporal regions (red spheres). Spheres in other colors represent nodes in different modules. Functional connections between nodes are represented with green lines. Abbreviations: IM, item memory; SM, source memory; MTL, medial temporal lobe. (For interpretation of the references to color in this figure legend, the reader is referred to the Web version of this article.)

Supporting our second premise, that the IM and SM networks contained a module that included most MTL nodes, both the IM and SM networks contained a single module that included all 6 MTL nodes (bilateral HC, anterior parahippocampal gyri, and posterior parahippocampal gyri). Nonetheless, these modules also included some nonMTL nodes, predominately consisting of surrounding temporal lobe regions, and we, therefore, call them *MTL+* modules. In addition to the MTL+ module, the IM network contained 3 other modules, which approximately corresponded to left frontoparietal, right frontoparietal, and visual modules. The SM network contained 4 other modules, which approximately corresponded to lateral frontoparietal, medial frontoparietal, anterior fusiform/inferior temporal gyrus, and visual modules.

Having shown that both the IM and SM networks are modular and contain an MTL+ module, we sought to corroborate our first prediction: *MTL module-inside functional connections would be similar for the IM and SM networks* (*shared network components*), *whereas MTL module-outside functional connections, particularly between the HC and LatPFC/PPC, would be stronger for SM than IM* (*distinct network components*). Consistent with our prediction, we found, statistically controlling for age group, statistically significant connection location (within vs. between MTL [see below in current section]) by memory type (IM, SM) interactions (all *z*'s > 2.96, *p*'s < 0.01; all measures were *z*-transformed). We further examined these interactions below; it should be noted that for any analysis describing participation coefficient results in a set of nodes (e.g., the 6 MTL nodes), participation coefficients were averaged across the nodes describing the region. Corroborating the first part of the prediction, between the IM and SM networks, the number of MTL-inside connections among the 6 MTL nodes was similar (Fig. 2A; $t\ [54] = -1.71$, $p = 0.093$). This result is consistent with our assumption that for IM and SM, functional connectivity *within* the MTL is similar (i.e., *shared* network components).

To examine if the SM compared to IM network had a greater number of MTL module-outside connections, we calculated the relative number of MTL+-outside to -inside connections (i.e., participation coefficients). As illustrated in Fig. 2B, compared to the IM network, within the SM network, nodes in the MTL+ module had higher participation coefficients ($p < 0.001$, permutation test). Moreover, this pattern persisted when focusing only on the 6 MTL nodes (Fig. 2C; $p < 0.01$, permutation test) and, intriguingly, was strongest when focusing only on the HC nodes (Fig. 2D; $p < 0.0001$, permutation test). Thus, within the SM network, MTL nodes contained more widespread functional connections to other brain regions that belonged to other modules in the network (i.e., *distinct* network components).

To further investigate MTL-outside connections, we focused on HC connections with LatPFC and PPC. Consistent with our prediction, the SM compared to IM network contained more HC-LatPFC (Fig. 3A; $t\ [54] = 2.38$, $p < 0.05$) and LatPFC-PPC connections (Fig. 3B; $t\ [54] = 2.09$, $p < 0.05$); the SM and IM networks, however, contained a similar number of HC-PPC connections ($t\ [54] = 0.00$, $p = 0.99$). These results further support the existence of an SM distinct network component.

3.3. Relation between functional properties of MTL+ modules and scaled RT

Our second prediction was that *after controlling for age, within the SM network, a greater proportion of MTL-outside than MTL-inside*

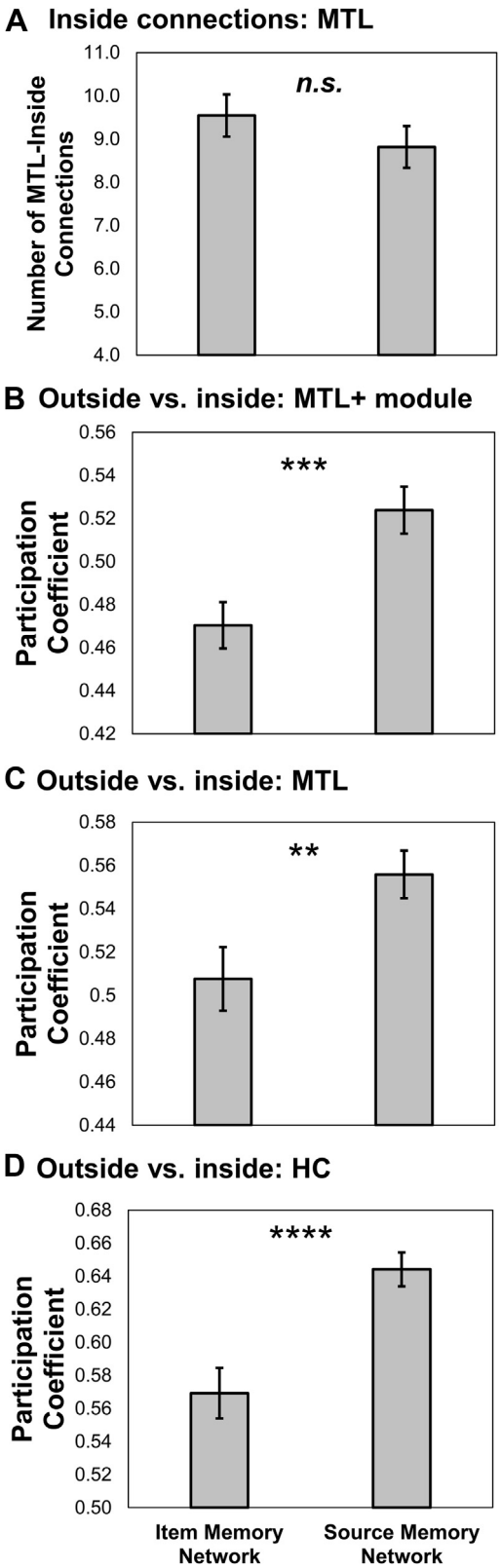

Fig. 2. Functional connections of the MTL+ module and HC in the IM and SM networks. Panel A shows that the number of functional connections among the 6 MTL nodes between the IM and SM networks was similar. Panels B, C, and D show that the relative number of outside versus inside functional connections (i.e., participation coefficients) for the whole MTL+ module, 6 MTL nodes, and HC, respectively, were greater in the SM than IM network. **** = $p < 0.0001$; *** = $p < 0.001$; ** = $p < 0.01$; Abbreviations: n.s., nonsignificant; error bars, standard error of the mean; IM, item memory; SM, source memory; MTL, medial temporal lobe; HC, hippocampus.

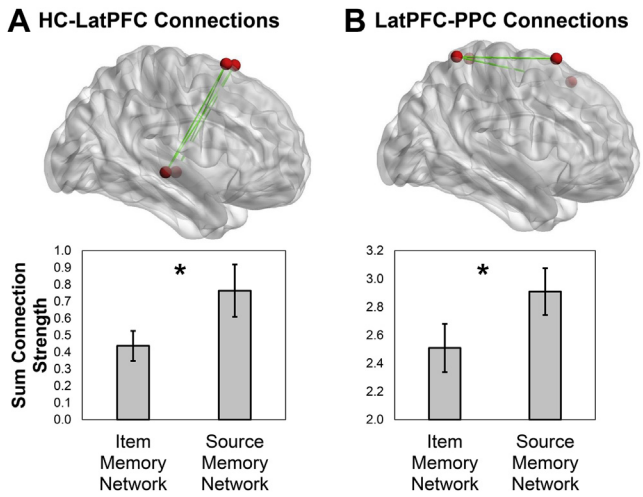

Fig. 3. Functional connections between HC, LatPFC, and PPC nodes in the IM and SM networks. Panel A shows that the average sum connection strength between the HC and LatPFC was greater in the SM than IM network. Likewise, Panel B shows that the average sum connection strength between the LatPFC and PPC was greater in the SM than IM network. Red spheres represent the center of mass of the nodes and green lines represent the functional connections between nodes. * = $p < 0.05$; error bars, standard error of the mean. Abbreviations: HC, hippocampus; IM, item memory; SM, source memory; MTL, medial temporal lobe; LatPFC, lateral prefrontal cortex; PPC, posterior parietal cortex. (For interpretation of the references to color in this figure legend, the reader is referred to the Web version of this article.)

connections (i.e., *greater participation coefficients*) *would be associated with greater SM task performance*. To test this prediction, we correlated SM and IM MTL+ participation coefficients with SM and IM scaled RTs (lower scaled RTs are indicative of greater efficiency), respectively; as described previously, we chose scaled RTs as the behavioral outcome measure to account for speed-accuracy tradeoffs (Boldini et al., 2007; Dosher, 1976; Horowitz and Wolfe, 2003; Madden et al., 2017; Smith and Brewer, 1995; Starns and Ratcliff, 2010; Townsend and Ashby, 1983). To reduce the possible influence of age, our analyses statistically controlled for age group. Supporting our second prediction, we found that scaled RT was significantly predicted by the memory type (IM, SM) by MTL+ participation coefficient interaction ($\beta = -11{,}352.7$, $z = -2.98$, $p < 0.01$), in which individuals with higher MTL+ participation coefficients had greater SM efficiency ($\beta = -11{,}305.2$, $z = -14.5$, $p < 0.0001$); this result was still statistically significant after controlling for potential outliers (via log-transforming participation coefficient and scaled RTs; $\beta = -0.8$, $z = -2.79$, $p < 0.01$; Fig. 4A). To examine the strength of this relation, we calculated the Pearson correlation coefficient between the log-transformed SM scaled RT and MTL+ participation coefficient (residualized for age group), which was −0.26. In contrast, in the IM network, this relation was weaker ($\beta = -752.5$, $z = -2.91$, $p < 0.01$) and not statistically significant after controlling for potential outliers (via log-transforming participation coefficient and scaled RTs; $\beta = 0.03$, $z = 0.25$, $p = 0.25$; Fig. 4B).

3.4. Age-related differences in the IM and SM networks

Our third prediction was that *the OAs* (*compared to YAs*), *in the SM network, would show more MTL module-outside than MTL module-inside connections* (i.e., *greater participation coefficients*). To test this prediction, we used age group–specific modules (see Section 2.4.3). We found that the IM and SM networks in both the YAs and OAs contained an MTL+ module consisting of all 6 MTL nodes and predominately surrounding temporal regions

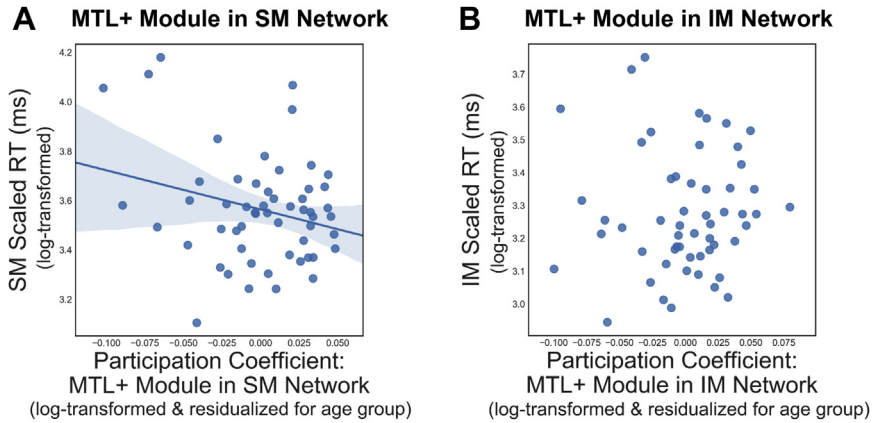

Fig. 4. Relation between outside versus inside connections and scaled RT in the SM and IM networks. Panel A shows that, controlling for age group, individuals with a greater proportion of outside than inside connections (i.e., higher participation coefficients) in the MTL+ module had lower SM-scaled RTs (greater efficiency). Panel B shows that this relation did not exist for the IM task. Both scaled RTs and participation coefficients are shown log-transformed and participation coefficients are partialled for age group. Abbreviations: RT, reaction time; IM, item memory; SM, source memory; MTL, medial temporal lobe.

(Supplementary Fig. 1). For each memory type (IM and SM) and age group (YA and OA) network, we estimated participation coefficients for the 6 MTL nodes. Supporting our prediction, we found a memory type by age group interaction ($\beta = 0.091$, $z = 2.66$, $p < 0.01$), in which, during SM, MTL participation coefficients were higher within the OAs than YAs ($p < 0.01$, permutation test; Fig. 5A), but, during IM, MTL participation coefficients were similar between the OAs and YAs ($p = 0.26$, permutation test; Fig. 5B). To determine the specificity of these findings, we compared, between the YAs and OAs, *Q*-values from the SM networks. We found that Q-values from the YAs ($M = 0.34$, *standard error* $= 0.02$) and OAs ($M = 0.33$, *standard error* $= 0.01$) were similar ($p = 0.25$, permutation test), suggesting that the more integrated network architecture for the OAs was specific to the MTL+ module.

4. Discussion

The overarching goal of the present study was to investigate shared and distinct network components underlying IM and SM retrieval within cognitively normal YAs and OAs. This study yielded 3 main findings. *First*, irrespective of age, MTL nodes were similarly interconnected among each other during both IM and SM (*shared* network components), whereas MTL nodes maintained more intermodule functional connections, especially with LatPFC/PPC nodes, during SM (*distinct* network components). *Second*, only within the SM network were MTL+ nodes with more widespread functional connections associated with better task performance. *Third*, in the SM network, OAs relative to YAs had MTL nodes with more widespread functional connections. These findings are discussed in greater detail in the following.

4.1. Modular architecture differences between the IM and SM networks

Our first question sought to examine within the IM and SM networks *shared* and *distinct* MTL functional connectivity patterns. Although univariate activation analyses have identified shared and distinct activation patterns (e.g., Giovanello and Schacter, 2012; Hayes et al., 2011; Spaniol et al., 2009; Vilberg and Rugg, 2007), this is the first study, to our knowledge, to characterize IM and SM components within a whole-brain network framework. We predicted that MTL module-inside connections would be similar within the IM and SM networks, whereas MTL module-outside connections (i.e., inter-MTL module connections), particularly between the HC and LatPFC/PPC, would be greater within the SM than IM network. As a first piece of evidence for the first part of our first prediction (*MTL-inside connections would be similar within the*

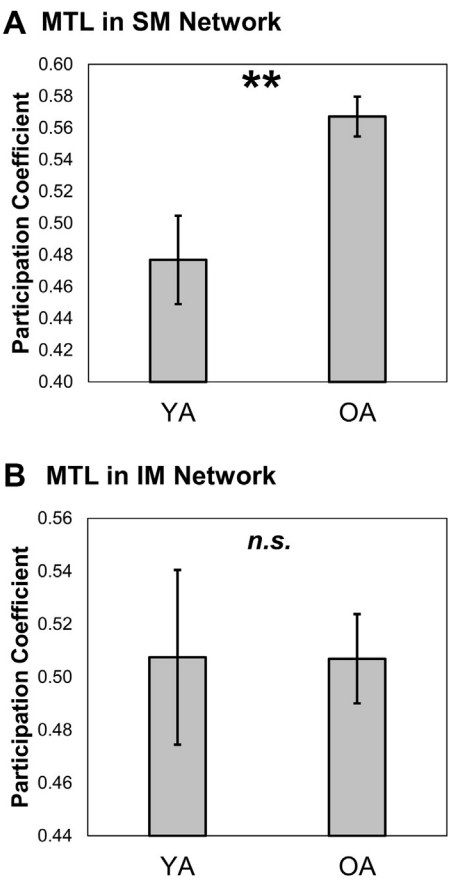

Fig. 5. Age-related differences in MTL-outside versus -inside connectivity in the SM and IM networks. Panel A shows that compared to the YAs, the OAs showed a greater proportion of MTL outside- versus inside-module connections (i.e., higher participation coefficients) in the SM network. Panel B shows that this was not true in the IM network. ** = $p < 0.01$; error bars, standard error of the mean. Abbreviations: IM, item memory; SM, source memory; MTL, medial temporal lobe; OAs, older adults; YAs, younger adults.

IM and SM networks), the modularity analysis revealed that both the IM and SM networks contained a single module that included all 6 MTL nodes (Fig. 1), which suggests the existence of a shared network component. We quantified the existence of this shared network component by examining IM versus SM within-MTL connections. Indeed, the IM versus SM networks contained a similar number of within-MTL connections (Fig. 2A), providing further support for the existence of a shared network component. As reviewed previously, several studies have demonstrated similar MTL activation during both IM and SM (e.g., Davachi et al., 2003; Hayes et al., 2011; Staresina and Davachi, 2008, 2009). Also, patients with MTL damage tend to be impaired in both IM and SM (e.g., Cipolotti and Bird, 2006; Holdstock et al., 2002; Huppert and Piercy, 1978; Nunn et al., 1999), further suggesting that the MTL is critical for both forms of memory. However, univariate activation and lesion evidence cannot ascertain the interactions among MTL subregions. Our results show that MTL regions are similarly interconnected among each other during both IM and SM, which further demonstrates the importance of examining functional connectivity to fully characterize the neural underpinnings of IM and SM. Modern memory theories state that the location of memory traces within neocortical regions are stored in the MTL (Alvarez and Squire, 1994; Buckner and Wheeler, 2001; Norman and O'Reilly, 2003). Although IM and SM traces are likely stored in different neocortical regions, according to these theories, both IM and SM would still use the MTL. Perhaps, our result of a shared network component reflects similar MTL interactions in service of retrieving the memory traces.

Regarding the second part of our first prediction (*MTL module-outside connections would be greater within the SM than IM network*), we found that the MTL+ module contained more outside than inside functional connections (i.e., higher participation coefficients) in the SM network (Fig. 2B); we also found this same pattern specifically with the 6 MTL nodes (Fig. 2C) and HC (Fig. 2D). Previous work has demonstrated that the HC becomes more integrated with the entire functional brain network to support the retrieval of vivid relative to dim memories of visual scenes (Geib et al., 2017b). Our finding of greater MTL integration in the SM relative to IM network may reflect SMs being more contextually rich. Supporting this interpretation, the strongest SM versus IM participation coefficient effect was within the HC (Fig. 2D).

Even further supporting the existence of an SM distinct network component, we found that the SM compared to IM network contained more HC-LatPFC and LatPFC-PPC functional connections (Fig. 3). Previous functional neuroimaging studies have shown that SM activates LatPFC and PPC regions (e.g., Cabeza et al., 2008; Dobbins et al., 2003; Giovanello and Schacter, 2012; Hayes et al., 2011; Kim, 2013; Spaniol et al., 2009; Vilberg and Rugg, 2007; Wheeler and Buckner, 2004), and lesion studies have shown that lesions in these regions impair SM (e.g., Ben-Zvi et al., 2015; Butters et al., 1994; Cabeza et al., 2008; Duarte et al., 2005; Janowsky et al., 1989; Simons et al., 2010). Also, preliminary evidence indicates that during SM, MTL regions are functionally connected to LatPFC and PPC (e.g., Foster et al., 2016; McCormick et al., 2010), but this literature is limited in that these studies have not directly compared SM to IM functional connectivity patterns. Our results expand this literature by demonstrating that the LatPFC interacts with the MTL more strongly during SM than during IM. Surprisingly, however, the SM and IM networks contained a similar number of PPC-HC connections. Although it cannot be definitively determined from these analyses, the PPC may be indirectly functionally connected with the HC via the LatPFC, as the SM network contained more HC-LatPFC and LatPFC-PPC functional connections. Overall, these findings are similar to previous network studies investigating LatPFC and PPC connectivity during SM retrieval (King et al., 2015; Schedlbauer et al., 2014; Wang et al., 2010; Watrous et al., 2013), but go beyond these studies by directly comparing connectivity between these regions and the MTL during SM and IM. Although our findings do not speak to the nature of the cognitive operations mediated by frontoparietal-MTL interactions during SM, the literature suggests they are likely to be executive function processes contributing to memory search and monitoring (Bunge et al., 2004; Cabeza et al., 2008; Dobbins et al., 2002).

In sum, our results indicate that the main difference between the SM and IM networks is not interactions among MTL regions (MTL-inside connections), but rather in the interactions between the MTL and inter-MTL+ module regions, especially frontoparietal regions (MTL-outside connections). It is only in the examination of functional interactions that process-specific alliances (PSAs; the interactions between component processes) may be investigated (Cabeza and Moscovitch, 2013; Moscovitch et al., 2016), which describe a set of regions communicating with each other in service of a cognitive process. PSAs are typically viewed as component interactions between 2 or 3 regions. Here, we investigated whole-brain functional networks, which allowed for the examination of multiple PSAs during IM and SM. Our results suggest that both IM and SM share a similar set of PSAs (reflected here as similar interactions within the MTL) and that SM uses additional PSAs (reflected here in inter-MTL connections). However, it should be noted that because our analyses focused on modules containing MTL nodes, similar or different PSAs during IM and SM may be underlain by brain regions not examined here. Future studies may attempt to identify other potential PSAs underlying IM and SM and the cognitive operations underlying these PSAs.

4.2. Relation between functional network properties and task performance

If SM and IM involve similar MTL-inside connections but SM involves greater MTL-outside connections, a natural question to ask is whether the emphasis on MTL-outside connections is important for SM performance. To investigate this question, we linked the relative number of MTL module-outside versus -inside connections to SM performance. Specifically, we tested the prediction that after controlling for age group, within the SM network, a greater proportion of MTL module-outside than MTL-inside connections (i.e., greater participation coefficients) would be associated with better SM performance. Consistent with this prediction, we found that in the SM network (Fig. 4A), but not in the IM network (Fig. 4B), there was a significant correlation between MTL+ participation coefficients and scaled RT, in which individuals with more MTL+-outside connections exhibited greater SM efficiency; however, it should be noted that the strength of the correlation was relatively weak.

These findings further indicate the importance of widely interconnected MTL+ nodes in service of SM and are consistent with past studies indicating that a more integrated functional network is associated with better performance on complex cognitive tasks (e.g., Barbey, 2018; Geib et al., 2017a,b; Grady et al., 2016; Meunier et al., 2014; Monge et al., 2017; Stanley et al., 2015). During IM, it does not appear that globally interconnected MTL+ nodes are important for task performance. Thus, our second finding extends the first finding by showing that the emphasis of SM on global interconnections is important for successful SM performance.

4.3. Age-related differences in the IM and SM networks

Finally, our last prediction examined age-related differences in the functional network properties underlying IM and SM retrieval. Because OAs show a greater deficit in SM than IM (for a review, see

Spencer and Raz, 1995), we predicted that these changes would be mostly present during SM. Consistent with our prediction, we found during SM that the MTL was more integrated within the OAs than YAs (Fig. 5A); this pattern was not present during IM (Fig. 5B). Many past studies have demonstrated that, compared to YAs, OAs exhibit more widespread activation patterns in service of episodic memory (for a review, see Cabeza and Dennis, 2013). This phenomenon has been attributed either to *compensation* (e.g., Cabeza, 2002; Cabeza et al., 1997; Reuter-Lorenz and Stanczak, 2000) or *dedifferentiation* (e.g., Li and Lindenberger, 1999). Here, we found evidence more strongly supporting the compensation hypothesis. First, we found during SM that the MTL nodes were more integrated within the OAs than YAs. Second, we found that better SM performance was associated with a more integrated MTL+ module; evidence for dedifferentiation would have shown that worse SM performance was associated with a more integrated MTL+ module. Finally, we found that *Q*-values between the YAs and OAs did not differ, suggesting that the more integrated network architecture for OAs was specific to the task-relevant MTL+ module.

Although compensation during episodic memory has been demonstrated in several univariate activation studies (for a review, see Cabeza and Dennis, 2013), this is the first study, to our knowledge, to demonstrate episodic memory–related compensation within the context of functional networks. Similar to our results, several other studies have demonstrated within other cognitive domains that aging is associated with a more integrated modular architecture in service of cognition (Chan et al., 2017; Gallen et al., 2016; Grady et al., 2016; Monge et al., 2017). Previous memory studies have demonstrated age-related increases in the interactions between sets of regions (i.e., bivariate functional connectivity; Dennis et al., 2008), but here we demonstrate that age-related increases in functional connectivity also occur at a more global scale. Our results and the findings of previous studies further motivate the importance of examining task-based functional networks to provide a novel framework characterizing mechanisms underlying cognitive aging.

4.4. Methodological considerations

Within the present study, we made several methodological choices that should be discussed. First, here, we had separate IM and SM tasks, which differs from some other studies assessing IM and SM in which participants' memory for the item was tested, and for stimuli indicated as old, the source test immediately followed (e.g., Cansino et al., 2002, 2015). We believe that there are advantages and disadvantages to both approaches. First, a disadvantage of the latter approach is that it entails a more complex decision process (e.g., switching across dimensions, setting of different decision criteria, etc.), which may introduce confounds. Second, the method used in the present study may be more sensitive to retrieval orientation, and retrieval orientation is an important component of retrieval that should be taken into consideration when examining the neural correlates of IM and SM. The advantages and disadvantages of both approaches should be considered during study design.

Another methodological consideration worth noting is the choice of atlas for defining nodes and the threshold implemented for the connectivity matrices. Different atlases and thresholds likely affect topological properties of brain networks, but there are no definitive standards in the field for the best atlas or best thresholding procedure (Stanley et al., 2013; Telesford et al., 2010, 2013). In fact, some have argued that the atlas and thresholding procedure implemented for any given study should be dependent on the research question (Stanley et al., 2013). Regarding the choice of atlas, we chose the Harvard-Oxford Atlas (Desikan et al., 2006) to better differentiate and investigate subregions of the MTL (6 MTL nodes), compared to the also commonly used automated anatomical labeling atlas (Tzourio-Mazoyer et al., 2002), which only contains 4 MTL nodes. Regarding the choice of threshold, in the present study, the matrices were thresholded using a procedure that controlled for edge density (density = 0.20; Hayasaka and Laurienti, 2010). We specifically chose this threshold and procedure for several reasons. First, prior research has indicated that when edge density is equal to or between 0.20 and 0.30, topological properties of brain networks are more likely to be reproducible (Telesford et al., 2013). Second, in our study, a density of 0.20 prevented the matrices from becoming severely fractured, and it is difficult to interpret and compare topological properties between networks that are fractured and networks that are not. Third, this thresholding procedure provided us with a way to control for edge density between networks, meaning that direct comparisons between IM and SM networks provide results that are more clearly and easily interpretable. Of course, comparing our results with other task-related network analyses should be done with caution, if different atlases and thresholding procedures were implemented.

5. Conclusions

In sum, this is, to our knowledge, the first study to examine in YAs and OAs the functional network topology underlying both IM and SM retrieval. We demonstrated that, irrespective of age, MTL nodes were similarly interconnected among each other during both IM and SM (*shared* network components), but MTL module nodes maintained more intermodular-functional connections, especially with LatPFC/PPC nodes, during SM (*distinct* network components). Also, we showed that only within the SM network were MTL+ nodes with more widespread functional connections associated with better task performance. Finally, we demonstrated that, compared to YAs, OAs had MTL nodes with more widespread functional connections in service of SM retrieval. Overall, our results provide a novel viewpoint on neural mechanism differences of processes supporting IM compared to SM in YAs and OAs by describing these mechanisms within the context of whole-brain functional networks.

Disclosure statement

The authors have no actual or potential conflicts of interest.

Acknowledgements

This work was supported by the National Institute on Aging (R01 AG019731 to RC). The funding agency had no role in the decision to publish or prepare the article.

Appendix A. Supplementary data

Supplementary data associated with this article can be found, in the online version, at https://doi.org/10.1016/j.neurobiolaging.2018.05.016.

References

Alvarez, P., Squire, L.R., 1994. Memory consolidation and the medial temporal lobe: a simple network model. Proc. Natl. Acad. Sci. U. S. A. 91, 7041–7045.
Backus, A.R., Bosch, S.E., Ekman, M., Grabovetsky, A.V., Doeller, C.F., 2016. Mnemonic convergence in the human hippocampus. Nat. Commun. 7, 11991.
Barbey, A.K., 2018. Network neuroscience theory of human intelligence. Trends Cogn. Sci. 22, 8–20.
Bassett, D.S., Wymbs, N.F., Porter, M.A., Mucha, P.J., Carlson, J.M., Grafton, S.T., 2011. Dynamic reconfiguration of human brain networks during learning. Proc. Natl. Acad. Sci. U. S. A. 108, 7641–7646.

Ben-Zvi, S., Soroker, N., Levy, D.A., 2015. Parietal lesion effects on cued recall following pair associate learning. Neuropsychologia 73, 176–194.
Betzel, R.F., Byrge, L., He, Y., Goñi, J., Zuo, X.-N., Sporns, O., 2014. Changes in structural and functional connectivity among resting-state networks across the human lifespan. Neuroimage 102, 345–357.
Blondel, V.D., Guillaume, J.L., Lambiotte, R., Lefebvre, E., 2008. Fast unfolding of communities in large networks. J. Stat. Mech. Theory Exp. 2008, P10008.
Boldini, A., Russo, R., Punia, S., Avons, S.E., 2007. Reversing the picture superiority effect: a speed-accuracy trade-off study of recognition memory. Mem. Cognit. 35, 113–123.
Bravo, G., Hébert, R., 1997. Age- and education-specific reference values for the Mini-Mental and Modified Mini-Mental State Examinations derived from a non-demented elderly population. Int. J. Geriatr. Psychiatry 12, 1008–1018.
Buckner, R.L., Wheeler, M.E., 2001. The cognitive neuroscience of remembering. Nat. Rev. Neurosci. 2, 624–634.
Bullmore, E., Sporns, O., 2009. Complex brain networks: graph theoretical analysis of structural and functional systems. Nat. Rev. Neurosci. 10, 186–198.
Bunge, S.A., Burrows, B., Wagner, A.D., 2004. Prefrontal and hippocampal contributions to visual associative recognition: interactions between cognitive control and episodic retrieval. Brain Cogn. 56, 141–152.
Butters, M.A., Kaszniak, A.W., Glisky, E.L., Eslinger, P.J., Schacter, D.L., 1994. Recency discrimination deficits in frontal lobe patients. Neuropsychology 8, 343–354.
Cabeza, R., 2002. Hemispheric asymmetry reduction in older adults: the HAROLD model. Psychol. Aging 17, 85–100.
Cabeza, R., Ciaramelli, E., Olson, I.R., Moscovitch, M., 2008. The parietal cortex and episodic memory: an attentional account. Nat. Rev. Neurosci. 9, 613–625.
Cabeza, R., Dennis, N.A., 2013. Frontal lobes and aging: deterioration and compensation. In: Stuss, D.T., Knight, R.T. (Eds.), Principles of Frontal Lobe Function, second ed. Oxford University Press, New York, pp. 628–652.
Cabeza, R., Grady, C.L., Nyberg, L., McIntosh, A.R., Tulving, E., Kapur, S., Jennings, J.M., Houle, S., Craik, F.I.M., 1997. Age-related differences in neural activity during memory encoding and retrieval: a positron emission tomography study. J. Neurosci. 17, 391–400.
Cabeza, R., Moscovitch, M., 2013. Memory systems, processing modes, and components: functional neuroimaging evidence. Perspect. Psychol. Sci. 8, 49–55.
Cansino, S., Estrada-Manilla, C., Trejo-Morales, P., Pasaye-Alcaraz, E.H., Aguilar-Castañeda, E., Salgado-Lujambio, P., Sosa-Ortiz, A.L., 2015. fMRI subsequent source memory effects in young, middle-aged and old adults. Behav. Brain Res. 280, 24–35.
Cansino, S., Maquet, P., Dolan, R.J., Rugg, M.D., 2002. Brain activity underlying encoding and retrieval of source memory. Cereb. Cortex 12, 1048–1056.
Chan, M.Y., Alhazmi, F.H., Park, D.C., Savalia, N.K., Wig, G.S., 2017. Resting-state network topology differentiates task signals across the adult life span. J. Neurosci. 37, 2734–2745.
Chan, M.Y., Park, D.C., Savalia, N.K., Petersen, S.E., Wig, G.S., 2014. Decreased segregation of brain systems across the healthy adult lifespan. Proc. Nat. Acad. Sci. U. S. A. 111, E4997–E5006.
Cipolotti, L., Bird, C.M., 2006. Amnesia and the hippocampus. Curr. Opin. Neurol. 19, 593–598.
Cohen, J.R., D'Esposito, M., 2016. The segregation and integration of distinct brain networks and their relationship to cognition. J. Neurosci. 36, 12083–12094.
Davachi, L., Mitchell, J.P., Wagner, A.D., 2003. Multiple routes to memory: distinct medial temporal lobe processes build item and source memories. Proc. Natl. Acad. Sci. U. S. A. 100, 2157–2162.
Davis, S.W., Luber, B., Murphy, D.L., Lisanby, S.H., Cabeza, R., 2017. Frequency-specific neuromodulation of local and distant connectivity in aging & episodic memory function. Hum. Brain Mapp. 38, 5987–6004.
Dennis, N.A., Hayes, S.M., Prince, S.E., Madden, D.J., Huettel, S.A., Cabeza, R., 2008. Effects of aging on the neural correlates of successful item and source memory encoding. J. Exp. Psychol. Learn Mem. Cogn. 34, 791–808.
Desikan, R.S., Ségonne, F., Fischl, B., Quinn, B.T., Dickerson, B.C., Blacker, D., Buckner, R.L., Dale, A.M., Maguire, R.P., Hyman, B.T., 2006. An automated labeling system for subdividing the human cerebral cortex on MRI scans into gyral based regions of interest. Neuroimage 31, 968–980.
Dobbins, I.G., Foley, H., Schacter, D.L., Wagner, A.D., 2002. Executive control during episodic retrieval: multiple prefrontal processes subserve source memory. Neuron 35, 989–996.
Dobbins, I.G., Rice, H.J., Wagner, A.D., Schacter, D.L., 2003. Memory orientation and success: separable neurocognitive components underlying episodic recognition. Neuropsychologia 41, 318–333.
Dosher, B.A., 1976. The retrieval of sentences from memory: a speed-accuracy study. Cogn. Psychol. 8, 291–310.
Duarte, A., Ranganath, C., Knight, R.T., 2005. Effects of unilateral prefrontal lesions on familiarity, recollection, and source memory. J. Neurosci. 25, 8333–8337.
Dulas, M.R., Duarte, A., 2012. The effects of aging on material-independent and material-dependent neural correlates of source memory retrieval. Cereb. Cortex. 22, 37–50.
Eichenbaum, H., Yonelinas, A., Ranganath, C., 2007. The medial temporal lobe and recognition memory. Ann. Rev. Neurosci. 30, 123–152.
Folstein, M.F., Folstein, S.E., McHugh, P.R., 1975. "Mini-mental state". A practical method for grading the cognitive state of patients for the clinician. J. Psychiatr. Res. 12, 189–198.
Fornito, A., Harrison, B.J., Zalesky, A., Simons, J.S., 2012. Competitive and cooperative dynamics of large-scale brain functional networks supporting recollection. Proc. Natl. Acad. Sci. U. S. A. 109, 12788–12793.
Foster, C.M., Picklesimer, M.E., Mulligan, N.W., Giovanello, K.S., 2016. The effect of age on relational encoding as revealed by hippocampal functional connectivity. Neurobiol. Learn Mem. 134, 5–14.
Francis, W.N., Kucera, H., 1967. Computational Analysis of Present-day American English. Brown University Press, Providence, Rhode Island.
Gallen, C.L., Turner, G.R., Adnan, A., D'Esposito, M., 2016. Reconfiguration of brain network architecture to support executive control in aging. Neurobiol. Aging 44, 42–52.
Geerligs, L., Renken, R.J., Saliasi, E., Maurits, N.M., Lorist, M.M., 2015. A brain-wide study of age-related changes in functional connectivity. Cereb. Cortex. 25, 1987–1999.
Geib, B.R., Stanley, M.L., Dennis, N.A., Woldorff, M.G., Cabeza, R., 2017a. From hippocampus to whole-brain: the role of integrative processing in episodic memory retrieval. Hum. Brain Mapp. 38, 2242–2259.
Geib, B.R., Stanley, M.L., Wing, E.A., Laurienti, P.J., Cabeza, R., 2017b. Hippocampal contributions to the large-scale episodic memory network predict vivid visual memories. Cereb. Cortex. 27, 680–693.
Giovanello, K.S., Schacter, D.L., 2012. Reduced specificity of hippocampal and posterior ventrolateral prefrontal activity during relational retrieval in normal aging. J. Cogn. Neurosci. 24, 159–170.
Grady, C.L., Sarraf, S., Saverino, C., Campbell, K., 2016. Age differences in the functional interactions among the default, frontoparietal control, and dorsal attention networks. Neurobiol. Aging 41, 159–172.
Guimera, R., Amaral, L.A.N., 2005. Functional cartography of complex metabolic networks. Nature 433, 895–900.
Hayasaka, S., Laurienti, P.J., 2010. Comparison of characteristics between region-and voxel-based network analyses in resting-state fMRI data. Neuroimage 50, 499–508.
Hayes, S.M., Buchler, N., Stokes, J., Kragel, J., Cabeza, R., 2011. Neural correlates of confidence during item recognition and source memory retrieval: evidence for both dual-process and strength memory theories. J. Cogn. Neurosci. 23, 3959–3971.
Holdstock, J.S., Mayes, A.R., Roberts, N., Cezayirli, E., Isaac, C.L., O'Reilly, R.C., Norman, K.A., 2002. Under what conditions is recognition spared relative to recall after selective hippocampal damage in humans? Hippocampus 12, 341–351.
Horowitz, T., Wolfe, J., 2003. Memory for rejected distractors in visual search? Vis. Cogn. 10, 257–298.
Huppert, F.A., Piercy, M., 1978. The role of trace strength in recency and frequency judgements by amnesic and control subjects. Q. J. Exp. Psychol. 30, 347–354.
Janowsky, J.S., Shimamura, A.P., Kritchevsky, M., Squire, L.R., 1989. Cognitive impairment following frontal lobe damage and its relevance to human amnesia. Behav. Neurosci. 103, 548–560.
Kim, H., 2013. Differential neural activity in the recognition of old versus new events: an activation likelihood estimation meta-analysis. Hum. Brain Mapp. 34, 814–836.
King, D.R., de Chastelaine, M., Elward, R.L., Wang, T.H., Rugg, M.D., 2015. Recollection-related increases in functional connectivity predict individual differences in memory accuracy. J. Neurosci. 35, 1763–1772.
Leshikar, E.D., Gutchess, A.H., Hebrank, A.C., Sutton, B.P., Park, D.C., 2010. The impact of increased relational encoding demands on frontal and hippocampal function in older adults. Cortex 46, 507–521.
Li, S.-C., Lindenberger, U., 1999. Cross-level unification: a computational exploration of the link between deterioration of neurotransmitter systems and dedifferentiation of cognitive abilities in old age. In: Lars-Göran, N., Markowitsch, H.J. (Eds.), Cognitive Neuroscience of Memory. Hogrefe & Huber Publishers, Ashland, OH, pp. 103–146.
Madden, D.J., Parks, E.L., Tallman, C.W., Boylan, M.A., Hoagey, D.A., Cocjin, S.B., Johnson, M.A., Chou, Y.H., Potter, G.G., Chen, N.K., Packard, L.E., Siciliano, R.E., Monge, Z.A., Diaz, M.T., 2017. Frontoparietal activation during visual conjunction search: effects of bottom-up guidance and adult age. Hum. Brain Mapp. 38, 2128–2149.
McCormick, C., Moscovitch, M., Protzner, A.B., Huber, C.G., McAndrews, M.P., 2010. Hippocampal–neocortical networks differ during encoding and retrieval of relational memory: functional and effective connectivity analyses. Neuropsychologia 48, 3272–3281.
Meunier, D., Fonlupt, P., Saive, A.-L., Plailly, J., Ravel, N., Royet, J.P., 2014. Modular structure of functional networks in olfactory memory. Neuroimage 95, 264–275.
Mišić, B., Sporns, O., 2016. From regions to connections and networks: new bridges between brain and behavior. Curr. Opin. Neurobiol. 40, 1–7.
Mitchell, K.J., Johnson, M.K., 2009. Source monitoring 15 years later: what have we learned from fMRI about the neural mechanisms of source memory? Psychol. Bull 135, 638–677.
Monge, Z.A., Geib, B.R., Siciliano, R.E., Packard, L.E., Tallman, C.W., Madden, D.J., 2017. Functional modular architecture underlying attentional control in aging. Neuroimage 155, 257–270.
Monge, Z.A., Wing, E.A., Stokes, J., Cabeza, R., 2018. Search and recovery of autobiographical and laboratory memories: shared and distinct neural components. Neuropsychologia 110, 44–54.
Moscovitch, M., Cabeza, R., Winocur, G., Nadel, L., 2016. Episodic memory and beyond: the hippocampus and neocortex in transformation. Annu. Rev. Psychol. 67, 105–134.
Norman, K.A., O'Reilly, R.C., 2003. Modeling hippocampal and neocortical contributions to recognition memory: a complementary-learning-systems approach. Psychol. Rev. 110, 611–646.
Nunn, J.A., Graydon, F.J.X., Polkey, C.E., Morris, R.G., 1999. Differential spatial memory impairment after right temporal lobectomy demonstrated using temporal titration. Brain 122, 47–59.

Reuter-Lorenz, P.A., Stanczak, L., 2000. Differential effects of aging on the functions of the corpus callosum. Dev. Neuropsychol. 18, 113–137.
Rubinov, M., Sporns, O., 2010. Complex network measures of brain connectivity: uses and interpretations. Neuroimage 52, 1059–1069.
Schedlbauer, A.M., Copara, M.S., Watrous, A.J., Ekstrom, A.D., 2014. Multiple interacting brain areas underlie successful spatiotemporal memory retrieval in humans. Sci. Rep. 4, 6431.
Schubert, A., 2013. Measuring the similarity between the reference and citation distributions of journals. Scientometrics 96, 305–313.
Schubert, A., Telcs, A., 2014. A note on the Jaccardized Czekanowski similarity index. Scientometrics 98, 1397–1399.
Seabold, S., Perktold, J., 2010. Statsmodels: econometric and statistical modeling with Python. In: Proceedings of the 9th Python in Science Conference, pp. 57–61.
Simons, J.S., Peers, P.V., Mazuz, Y.S., Berryhill, M.E., Olson, I.R., 2010. Dissociation between memory accuracy and memory confidence following bilateral parietal lesions. Cereb. Cortex 20, 479–485.
Simpson, S., Lyday, R., Hayasaka, S., Marsh, A., Laurienti, P., 2013. A permutation testing framework to compare groups of brain networks. Front. Comput. Neurosci. 7, 171.
Skinner, E.I., Fernandes, M.A., 2007. Neural correlates of recollection and familiarity: a review of neuroimaging and patient data. Neuropsychologia 45, 2163–2179.
Smith, G.A., Brewer, N., 1995. Slowness and age: speed-accuracy mechanisms. Psychol. Aging 10, 238–247.
Spaniol, J., Davidson, P.S.R., Kim, A.S.N., Han, H., Moscovitch, M., Grady, C.L., 2009. Event-related fMRI studies of episodic encoding and retrieval: meta-analyses using activation likelihood estimation. Neuropsychologia 47, 1765–1779.
Spaniol, J., Grady, C., 2012. Aging and the neural correlates of source memory: over-recruitment and functional reorganization. Neurobiol. Aging 33, 425.e3–425.e18.
Spencer, W.D., Raz, N., 1995. Differential effects of aging on memory for content and context: a meta-analysis. Psychol. Aging 10, 527–539.
Sporns, O., Betzel, R.F., 2016. Modular brain networks. Annu. Rev. Psychol. 67, 613–640.
Stanley, M.L., Brigard, F.D., 2016. Modularity in network neuroscience and neural reuse. Behav. Brain Sci. 39, e133.
Stanley, M.L., Dagenbach, D., Lyday, R.G., Burdette, J.H., Laurienti, P.J., 2014. Changes in global and regional modularity associated with increasing working memory load. Front. Hum. Neurosci. 8, 954.
Stanley, M.L., Moussa, M.N., Paolini, B.M., Lyday, R.G., Burdette, J.H., Laurienti, P.J., 2013. Defining nodes in complex brain networks. Front Comput. Neurosci. 7, 169.
Stanley, M.L., Simpson, S.L., Dagenbach, D., Lyday, R.G., Burdette, J.H., Laurienti, P.J., 2015. Changes in brain network efficiency and working memory performance in aging. PLoS One 10, e0123950.
Staresina, B.P., Davachi, L., 2008. Selective and shared contributions of the hippocampus and perirhinal cortex to episodic item and associative encoding. J. Cogn. Neurosci. 20, 1478–1489.
Staresina, B.P., Davachi, L., 2009. Mind the gap: binding experiences across space and time in the human hippocampus. Neuron 63, 267–276.
Starns, J.J., Ratcliff, R., 2010. The effects of aging on the speed-accuracy compromise: boundary optimality in the diffusion model. Psychol. Aging 25, 377–390.
Telesford, Q.K., Burdette, J., Laurienti, P., 2013. An exploration of graph metric reproducibility in complex brain networks. Front. Neurosci. 7, 67.
Telesford, Q.K., Morgan, A.R., Hayasaka, S., Simpson, S.L., Barret, W., Kraft, R.A., Mozolic, J.L., Laurienti, P.J., 2010. Reproducibility of graph metrics in fMRI networks. Front. Neuroinformatics 4, 117.
Telesford, Q.K., Simpson, S.L., Burdette, J.H., Hayasaka, S., Laurienti, P.J., 2011. The brain as a complex system: using network science as a tool for understanding the brain. Brain Connect 1, 295–308.
Townsend, J., Ashby, F., 1983. The Stochastic Modeling of Elementary Psychological Processes. Cambridge University Press, Cambridge.
Tzourio-Mazoyer, N., Landeau, B., Papathanassiou, D., Crivello, F., Etard, O., Delcroix, N., Mazoyer, B., Joliot, M., 2002. Automated anatomical labeling of activations in SPM using a macroscopic anatomical parcellation of the MNI MRI single-subject brain. Neuroimage 15, 273–289.
van den Heuvel, M.P., Sporns, O., 2013. Network hubs in the human brain. Trends Cogn. Sci. 17, 683–696.
van den Heuvel, M.P., Stam, C.J., Kahn, R.S., Hulshoff Pol, H.E., 2009. Efficiency of functional brain networks and intellectual performance. J. Neurosci. 29, 7619–7624.
Vilberg, K.L., Rugg, M.D., 2007. Dissociation of the neural correlates of recognition memory according to familiarity, recollection, and amount of recollected information. Neuropsychologia 45, 2216–2225.
Vilberg, K.L., Rugg, M.D., 2008. Memory retrieval and the parietal cortex: a review of evidence from a dual-process perspective. Neuropsychologia 46, 1787–1799.
Wais, P.E., 2008. fMRI signals associated with memory strength in the medial temporal lobes: a meta-analysis. Neuropsychologia 46, 3185–3196.
Wang, J.H., Zuo, X.N., Gohel, S., Milham, M.P., Biswal, B.B., He, Y., 2011. Graph theoretical analysis of functional brain networks: test-retest evaluation on short- and long-term resting-state functional MRI data. PLoS One 6, e21976.
Wang, L., Metzak, P.D., Honer, W.G., Woodward, T.S., 2010. Impaired efficiency of functional networks underlying episodic memory-for-context in schizophrenia. J. Neurosci. 30, 13171–13179.
Watrous, A.J., Tandon, N., Conner, C.R., Pieters, T., Ekstrom, A.D., 2013. Frequency-specific network connectivity increases underlie accurate spatiotemporal memory retrieval. Nat. Neurosci. 16, 349–356.
Wheeler, M.E., Buckner, R.L., 2004. Functional-anatomic correlates of remembering and knowing. Neuroimage 21, 1337–1349.
Wixted, J.T., 2007. Dual-process theory and signal-detection theory of recognition memory. Psychol. Rev. 114, 152–176.
Xia, M., Wang, J., He, Y., 2013. BrainNet Viewer: a network visualization tool for human brain connectomics. PLoS One 8, e68910.